

GRIDDED AEROSOL OPTICAL DEPTH CLIMATOLOGICAL DATASETS OVER CONTINENTS FOR SOLAR RADIATION MODELING

Christian A. Gueymard
Solar Consulting Services
97 Lake Fairgreen Circle
New Smyrna Beach, FL 32168
Chris@SolarConsultingServices.com

Ray George
National Renewable Energy Laboratory
1617 Cole Boulevard
Golden, CO 80401
Ray_George@nrel.gov

ABSTRACT

A methodology for the development of gridded datasets of aerosol optical depth (AOD) over continents is presented. This study focuses on the AOD at 550 nm and the Ångström turbidity coefficients α and β determined from spectral data, e.g., by sunphotometers. A method to derive the broadband AOD from the air mass, α and β , is proposed. Different satellite-based datasets (AVHRR, MISR and MODIS-GOCART) are used to develop monthly-average AOD relative to their respective grid resolution. Corrections are made in regions where incorrect or missing AOD values are found. Moreover, a special interpolation/resampling technique is used to generate broadband AOD maps at a final resolution of $0.1 \times 0.1^\circ$ (about 10 km x 10 km), taking into account the altitude effect on AOD. The resulting maps are being used to predict irradiance over Africa, America and Asia, with the appropriate solar radiation models.

1. INTRODUCTION

Aerosol optical depth (AOD) is a key spectral variable affecting solar radiation. It is a primary measure of how aerosols reduce direct beam radiation and increase diffuse radiation, particularly under clear skies. In most arid/desert areas, the solar resource (driven by direct irradiance) is high, but also highly sensitive to AOD because of this attenuating effect of aerosols on direct irradiance.

For any country desiring to maximize solar energy production, it is of vital importance to rely on solar radiation maps with sufficient spatial resolution and accuracy. Due to the lack of measured radiation data, this can only be achieved through intensive modeling. Any attempt at mapping the solar resource is therefore dependent on the availability of high-resolution data for each of the main variables influencing solar radiation: cloudiness, AOD, water vapor, ozone, site pressure and ground albedo. From this list, AOD

is the one that still resists accurate and spatially dense determination—at least over continents, where most solar applications reside.

Because AOD is highly variable in space and time, daily data are desirable with a resolution of 10 km or better. This, however, is not easily achievable yet due to the various limitations (accuracy and short history) in current data. Our current goal is to develop a gridded *climatology* of AOD, i.e., mean monthly data hopefully representative of the long-term situation.

This paper presents a description of the ongoing work aimed at developing such datasets that is undertaken by the National Renewable Energy Laboratory (NREL) with the help of subcontractors and other institutions. NREL is engaged in the production of solar radiation resource maps and datasets (and therefore the underlying AOD datasets) for various projects, such as UNEP's Solar and Wind Energy Resource Assessment (SWERA, <http://swera.unep.net>) [1], and NREL's own National Solar Radiation Data Base (NSRDB), which is now being updated and improved [2]. Whereas the latter is limited to the USA, the former project involves solar resource mapping over Africa, Central and South America, and Asia.

2. SOURCES OF DATA

Because of the importance of aerosols in the current global climate change context, the science of aerosol measurement and modeling is rapidly progressing. In particular, ground-based sunphotometer networks (mainly NASA's AERONET, <http://aeronet.gsfc.nasa.gov>) have been instituted to measure AOD at an increasing number of sites in the world with good accuracy. Concurrently, spectral instruments have been launched onboard various satellites to measure AOD with high spatial resolution (e.g., AVHRR, MODIS and MISR). Finally, chemical transport models (e.g., GOCART) have been developed to simulate the distribution of aerosols

over the world, along with their AOD at various time scales. Advanced statistical procedures have allowed a synergistic assimilation of data from these different sources, out of which the MODIS-GOCART dataset [3] was obtained. None of these data sources has all the necessary characteristics usually needed (accuracy, spatial resolution and long-term data). Therefore, several such sources need to be used concurrently, with interpolation, extrapolation and correction wherever needed. In particular, it has been found, in the course of this work and elsewhere (e.g., [4]), that both the MODIS-GOCART and MISR datasets had areas with excessively high or low AOD, due to cloud interference, ground albedo miscalculation, instrumental problems or retrieval algorithm shortcomings. Some outliers can be easily detected (e.g., extremely large AOD amidst areas known to be normally clean) and have been duly corrected. Validation exercises using ground-truth data (e.g., [5-7]) show that satellite-based datasets can contain large errors in AOD, albeit generally not large enough to become obvious outliers. Correction of such errors is difficult and will not be practical until refined retrieval algorithms, longer datasets, thorough validation, and instrumental redundancy become available. Hence, the gridded AOD datasets developed here must be considered as preliminary only.

TABLE 1: SUNPHOTOMETRIC DATA BASE

Continent	No. Sites	Avg. No. Months per Site	Avg. τ_{a550}	Avg. α
Africa	64	15.0	0.399	1.00
North America	135	19.6	0.145	1.14
Central & South America	72	12.8	0.497	1.25
Asia	20	16.2	0.381	1.08

AERONET data have been used extensively here (237 sites) because of their overall better accuracy, spectral resolution, geographic coverage, and longer records than any other source of global data over continents. The older sites of this network already provide climatological data of the highest value in various applications [8]. Data from 54 other sunphotometric sites have been added to improve analyses. An overall description of the ground-based datasets used here, broken down by continent, is provided in Table 1. Many sunphotometric sites are located close to strong aerosol sources, such as desert areas in Africa and Asia, or biomass burning areas in Africa and South America, hence the possible bias in the apparent larger average AOD for these continents than for North America.

Although a relatively large number of sites have been considered, many of them provided data for only a few months to a few years. Ideally, an aerosol climatology should be based on datasets spanning 10 to 30 years, or 120–360 months. The average number of data months per site (third column of Table 1) is considerably lower than this ideal

minimum requirement. This would not be too much of a problem if the year-to-year AOD variability were low or predictable. This, unfortunately, is not the case, as can be seen from Fig. 1, where mean monthly data from one site are displayed for nine years. Natural variability is compounded by the variable frequency in exceptional haziness (caused by volcanic eruptions, large forest fires, sand/dust storms or pollution episodes). This variability in turn causes inconsistency in the global dataset because all sites have not collected data during a unique, common period. For all these reasons, caution must be exerted when using global AOD datasets such as those presented here.

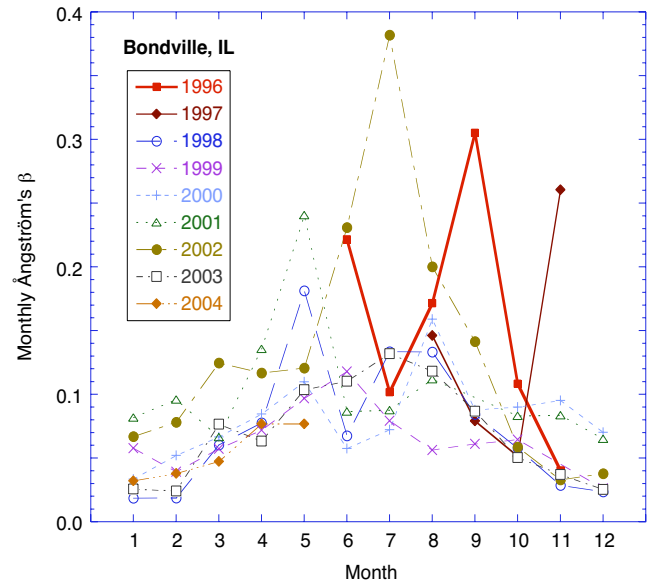


Fig. 1: Interannual variations of β at Bondville, Illinois.

3. REDUCTION OF DATA

3.1 Ground-based sunphotometric data

Ground-based sunphotometers measure the total optical depth of the atmosphere, τ_λ , at a few (usually 3–10) narrow-band channels of central wavelength λ . For each channel, the spectral AOD at wavelength λ , $\tau_{a\lambda}$, is obtained as τ_λ minus the sum of the spectral optical depths due to Rayleigh scattering and gaseous absorption [9, 10].

All AERONET sites are equipped with a Cimel sunphotometer, whose characteristics, performance, and calibration issues are described elsewhere [11]. This tracking instrument normally has eight channels. Seven of them are used to derive AOD between 340 and 1020 nm, and one (at 940 nm) is used to evaluate precipitable water. All-weather measurements are made automatically every 15 minutes or less, for values of air mass, m , below 7. A sophisticated post-processing algorithm allows the removal of cloud interfer-

ence [12]. (It is these authors' experience, based on manual inspection of the raw data, that the cloud-screening algorithm sometimes fails to detect and reject a few "slightly cloudy" data points; this source of error is assumed to not significantly affect the AOD results.)

Daily Level-2 (cloud-screened and quality-assessed) AOD data are used as follows. From the aerosol channels normally available, only data in the spectral range 380–1020 nm are considered here because of the frequent curvature of the $\tau_{a\lambda} = f(\lambda)$ function in the UV, in a spectral region where irradiance is relatively small. Using the AOD for these remaining channels (six at most) simultaneously, the Ångström turbidity factor, β , and wavelength exponent, α , are calculated by linearly fitting these data points to the log-log transform of Ångström's equation:

$$\ln \tau_{a\lambda} = \ln \beta - \alpha \ln(\lambda/\lambda_0), \quad (1)$$

where $\lambda_0 = 1000$ nm is the defining reference wavelength for β . Additionally, the AOD at 550 nm, τ_{a550} , is calculated for further reference and compatibility with other datasets (see Section 3.4), using $\lambda = 550$ nm in

$$\tau_{a\lambda} = \beta (\lambda/\lambda_0)^{-\alpha}. \quad (2)$$

An analysis of the relative frequency of daily values of β shows that they follow a log-normal probability distribution, thus confirming previous findings [13]. Figure 2 illustrates this behavior for a rural site subjected to frequent episodes of transported pollution (Bondville, Illinois) and a relatively clean, high-altitude city (Boulder, Colorado). The latter site clearly experiences more frequent occurrences of clean conditions (low AOD) than the former. From a statistical perspective, it is important to note that, for any climatic condition, the frequency distributions are highly skewed toward the left (low AOD). Contrarily to what would happen if AOD followed a normal (Gaussian) distribution, the arithmetic mean, median and mode are not co-located. As a result, the arithmetic mean—the most commonly reported statistic, and the only one that will be discussed here for conciseness—can be misleadingly high when using it instead of the *mode* for applications that call for the *most frequent* turbidity conditions at a given site.

All daily values are converted to monthly averages, and then to long-term monthly averages, provided that a minimum of three data days per month are available. Furthermore, data from the years 1993 and 1994 are excluded whenever advisable to avoid contamination from the Pinatubo effect.

Considerable year-to-year AOD variability is found at most sites, as exemplified in Fig. 1. This variability contributes to that in direct and diffuse irradiance because AOD is the main variable affecting them under clear skies. Moreover, it is also an important source of inconsistency when comparing the AOD climatologies from different sites with non-coincident measurement periods, as is the general case here.

The statistical caveats just discussed need to be kept in mind when using any of the current AOD global datasets.

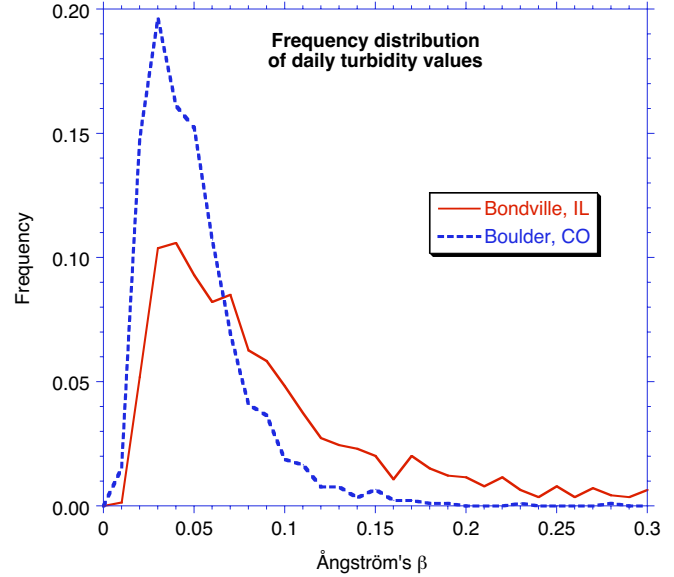


Fig. 2: Frequency distribution of β at Bondville, Illinois and Boulder, Colorado.

3.2 Conversion of spectral data to broadband AOD

Equation (2) can be used to evaluate $\tau_{a\lambda}$ from β and α at any wavelength. However, some radiation models, such as METSTAT [14], do not rely on spectral AOD information but on the *broadband* AOD (BAOD), τ_a , also known as the Unsworth-Monteith turbidity coefficient. So far, τ_a was usually derived from measurements of clear-sky direct irradiance and inversion of this type of model [15]. Because of the noticeable uncertainty in the resulting τ_a (due to the difficulties of selecting clear-sky radiation conditions *a posteriori*, uncertainties in concomitant precipitable water, etc.), and the scarcity of direct irradiance data, a less restricted and time-consuming derivation of τ_a is desirable. The simple concept of *effective wavelength* is useful in this respect [16, 17]. A direct correspondence between $\tau_{a\lambda}$ and τ_a exists for some effective wavelength, λ_e , such that:

$$\tau_a = \tau_{a\lambda_e} = \beta (\lambda_e/\lambda_0)^{-\alpha}. \quad (3)$$

To obtain λ_e as a solution of (3), the two-band REST2 model [18] can be run for a large number of ideal conditions for a wide range of (m , α , β) combinations. The broadband aerosol transmittance, T_a , and the corresponding broadband AOD, $\tau_a = -\ln(T_a)/m$ are then determined for each case. Using REST2's band-integrated effective-wavelength methodology, but in this case extended to the full shortwave spectrum, 0.29–4 μm , an accurate parameterization of λ_e is obtained from:

$$\lambda_e = (a_0 + a_1\beta)/(1 + a_2\beta) \quad (4)$$

$$a_0 = (0.71626 - 0.061545m + 6.182E-3m^2 - 1.6967E-6m^3)/(1 - 0.085406m + 8.6571E-3m^2) \quad (5a)$$

$$a_1 = (-0.11882 - 0.041746m + 0.074311m^2)/(1 + 0.3331m + 1.3131E-4m^2) \quad (5b)$$

$$a_2 = (-0.099397 - 0.35748m + 0.095173m^2 - 1.0801E-3m^3)/(1 + 0.76019m + 2.5629E-4m^2). \quad (5c)$$

Given monthly-average values of τ_{a550} and α , the monthly-average value of τ_a is calculated for each grid cell using a monthly-average value of m applied to (5). This in turn is calculated with an analytic method using only the site's latitude and the monthly-average sun's declination [19].

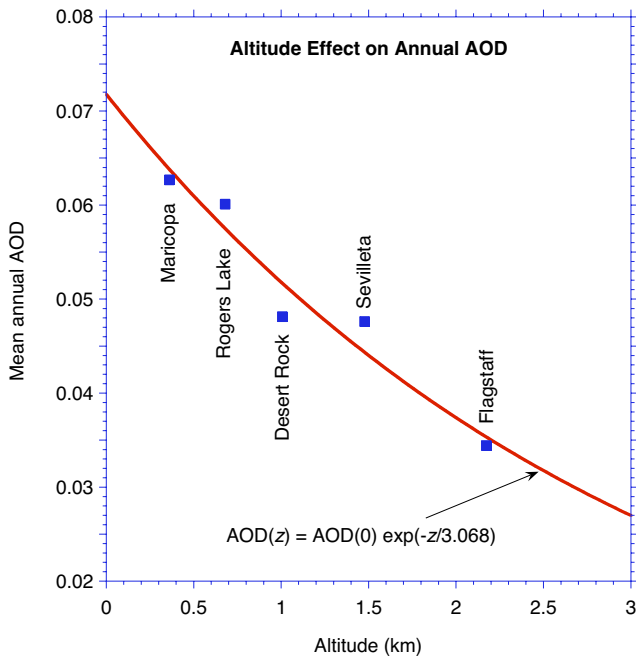


Fig. 3: Average AOD vs site altitude in the southwest USA.

3.3 Altitude effect

For reasons discussed in Section 3.5, it is useful to study the variation of AOD with altitude. It is known that, on average, AOD tends to decrease exponentially with altitude in the *free troposphere*. For instance, the classic Elterman aerosol model [20] implies that AOD decreases with altitude z as $\exp(-z/H)$ in the lower troposphere. The aerosol scale height, H , has been found to have a representative average of 1.2 km [20, 21], although far larger values have been found under highly stratified aerosol conditions [22]. The comparison of AOD over close-by sites whose altitude above sea level is significantly different may be a completely different issue, due in particular to rapid local and temporal changes in the convective boundary layer. Related fundamental studies have started only recently [23]. Useful

in situ experimental AOD measurements are still rare. Two widely different experiments carried out in the Alps have shown that an exponential decay law could be considered, as in the free troposphere case, but that the value of H was dependent on local and meteorological factors. Its average value was calculated to be 2.38 km between two sites in Germany [24], and was found to vary seasonally in Switzerland, most frequently between 0.5 and 2 km [25]. A similar approach has been used for the present study with sunphotometric data at five unpolluted sites in the southwest USA, ranging in altitude from 361 to 2173 m (Fig. 3). Using annual averages, a value $H = 3.068$ km has been found, leading to a reduction in AOD of 50% at an elevation of 2000 m compared to sea level.

3.4 Satellite-based spectroradiometric data

Three distinct satellite datasets have been considered for this investigation. The Global Aerosol Climatology Project (GACP, <http://gacp.giss.nasa.gov>) provides data of τ_{a550} and α from AVHRR [26]. These monthly means are available on a $1^\circ \times 1^\circ$ grid for a long period (7/1983–9/2001), but over water surfaces only. (The Pinatubo effect has been dealt with by excluding the period 6/1991–8/1994.) The more recent MISR instrument [27] observes the atmosphere at multiple angles on each path. Monthly mean values of τ_{a550} are available on a 0.5° global grid for the period 3/2000–11/2003, with some missing months. Finally, the MODIS-GOCART dataset [3] provides a worldwide τ_{a550} map on a $2.5^\circ \times 2^\circ$ grid, and covers the period 11/2000–10/2001. The GACP data are used for coastal locations only. MISR data are used primarily for Africa, and to prepare AOD maps at 31 U.S. test sites chosen for the validation of various radiation models [28]. The MODIS-GOCART dataset has been primarily used for all other mapping needs, but future improvements will rather rely on finer-resolution MISR and MODIS data.

Although the satellite instruments mentioned above are measuring AOD at different wavelengths (36 for MODIS, 4 for MISR, and 2 for AVHRR), only their results for 550 nm, τ_{a550} , were available when this study started. This prevented the use of the same methodology as in Section 3.1 to obtain α and β directly, except for AVHRR. A stop-gap procedure was therefore needed, and was developed from the observation that the geographical and temporal variations of α are, on average, more limited than those of AOD. They are, however, still too large to be represented by the common value of 1.3, which is typical of rural aerosols only. An analysis of the mean-monthly τ_{a550} and α data (from Section 3.1) shows a relatively good correlation between them, albeit specific to each continent. In particular, seasonal correlations can be isolated separately for the inland and coastal sites of Asia. For the U.S., where sunphotometric data are more abundant, a rough climatology of α has been obtained spatially for each month, using interpolation techniques. For

each grid cell, the τ_{a550} value from MODIS or MISR can be associated with the estimated α value to obtain β and τ_a through Eqs. (2)–(5).

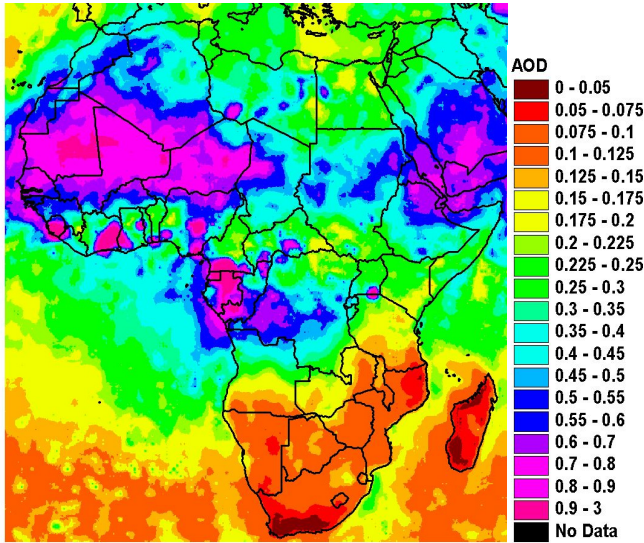


Fig. 4: Average τ_{a550} for June over Africa, based on MISR.

3.5 Turbidity mapping: final steps and products

An intricate method using Geographical Information System (GIS) software has been devised to resolve two problems at the same time: (i) the non-matching spatial resolution between all aerosol data sources and the other data requested by solar radiation models (cloudiness, water vapor, ozone and ground albedo), with a desired end resolution of $0.1 \times 0.1^\circ$, and (ii) the dependence of AOD on elevation, which is itself gridsizedependent information.

The current method works as follows. All input sources of AOD are assigned the appropriate terrain elevation. For gridded data sources, this is the mean elevation over the grid cell, averaged from 1-km resolution digital elevation data. For point observations, the station elevation is used. AOD data from point and grid locations are then converted to τ_a using the methodology in Section 3.2. This BAOD is adjusted to sea level using the empirical altitude function illustrated in Fig. 3. The sea-level BAOD is then interpolated to match the desired model grid. Where station data and gridded data are combined, some data points must be removed or subjectively edited, to allow the interpolation software to create the most realistic grid of τ_a . Finally, τ_a is adjusted back from sea level to the local elevation using the inverse exponential altitude adjustment.

An example of monthly-mean distribution of τ_{a550} over Africa based on MISR data is shown in Fig. 4. For this map, grid cells with missing data (from cloudy equatorial regions) were interpolated using a nearest-neighbor algorithm. The high aerosol load over western Africa, resulting from in-

tense sand storm and biomass burning activity in this period, is particularly visible. It is in striking contrast with the very low AOD prevalent over Madagascar and the southern tip of Africa, due to higher elevations and oceanic influences.

Figure 5 shows a similar map, but for τ_a over Asia in April, when powerful dust storms originating mostly from China's deserts are very frequent. This map was created by combining τ_{a550} from MODIS-GOCART on a 280-km grid with estimated α values (using the correlation explained above), and applying Eqs. (3)–(5). Both τ_{a550} and α in offshore regions come from the GACP data set.

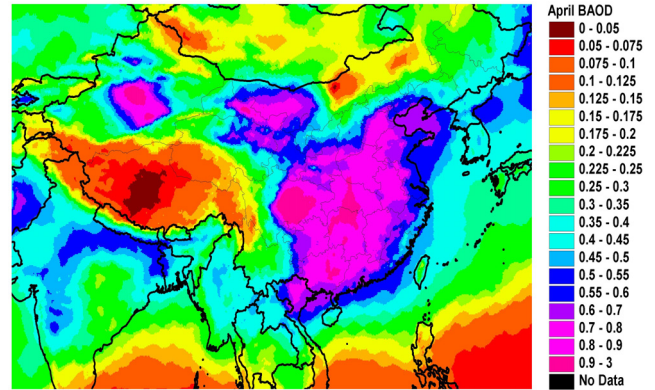


Fig. 5: Average τ_a for April over Asia, based on MODIS-GOCART.

Numerous sources of pollution also exist in eastern China and parts of India in particular, creating intense haze over most of the continent. All these aerosol clouds can cross the Indian Ocean or the Pacific Ocean. In the latter case, these dust clouds often yield elevated AOD over western North America in April and May, as can be inferred from Fig. 6. (Incidentally, these long-range transport episodes have a temporal impact on the solar resource [29].)

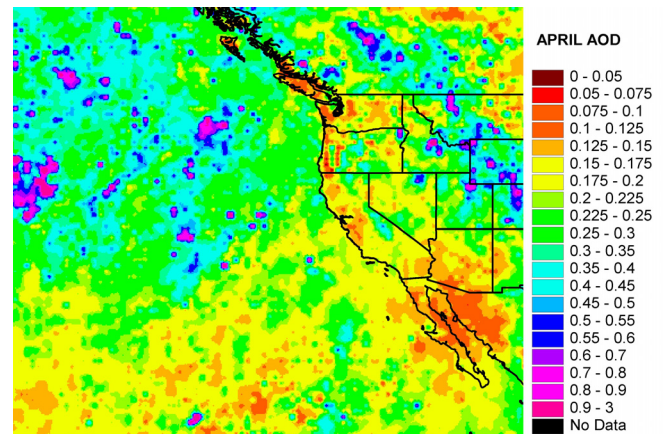


Fig. 6: MISR's average τ_{a550} for April, when Asian dust often crosses the Pacific and reaches North America.

Figure 7 shows monthly-average α from AERONET surface stations in southern California, interpolated to a 0.1° (≈ 10 km) grid. Values < 1.0 correspond to sea salt aerosols (La Jolla) and mineral dust (Owens Lake). In contrast, the strong urban smog of the Los Angeles basin usually results in values well above 1.3 (UCLA and MISR-JPL).

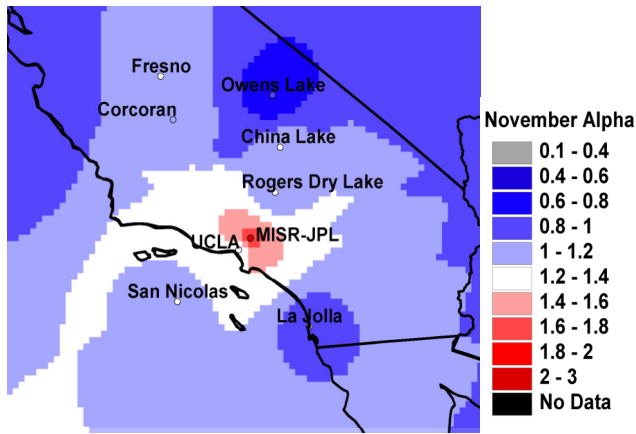


Fig. 7: Average α for November over Southern California.

4. CONCLUDING REMARKS

Any solar radiation model that uses either spectral AOD information (through α and either τ_{a550} or β) or broadband information (through τ_a) can directly benefit from the datasets and maps described here. The spatial resolution of the final products (≈ 10 km \times 10 km) is sufficient for most applications. Considerable resources, however, will be necessary to improve the synergy between ground data and satellite data (whose accuracy is still not up to par), and to obtain true gridded climatologies of α , β , τ_{a550} and τ_a . Subject to funding limitations, the data can be made available to interested researchers through the second author.

5. ACKNOWLEDGMENTS

This work was performed for the Department of Energy at the National Renewable Energy Laboratory under contract number DE-AC36-99GO10337. The AERONET staff and participants are thanked for their successful effort in establishing and maintaining all the sites whose datasets were pivotal to this study.

5. REFERENCES

(1) Renné D., et al., *Results of Solar Resource Assessments in the UNEP/SWERA Project*, Proc. Solar World Congress, International Solar Energy Society, 2005.

(2) Wilcox S., et al., *Progress on an updated National Solar Radiation Data Base for the United States*, Proc. Solar World Congress, International Solar Energy Society, 2005.

(3) Yu H., et al., *J. Geophys. Res.* **108D**, doi:10.1029/2002JD002717, 2003.

(4) Liu Y., et al., *J. Geophys. Res.* **109D**, doi:10.1029/2004JD005025, 2004.

(5) Kinne S., et al., *J. Geophys. Res.* **108D**, doi:10.1029/2001JD001253, 2003.

(6) Liu Y., et al., *J. Geophys. Res.* **109D**, doi:10.1029/2003JD003981, 2004.

(7) Chu D.A., et al., *Geophys. Res. Lett.* **29**, doi:10.1029/2001GL013205, 2002.

(8) Holben B.N., et al., *J. Geophys. Res.* **D106**, 12067-12097, 2001.

(9) Gueymard C.A. and Kambezidis H.D., *Solar spectral radiation, in Solar Radiation and Daylight Models*, T. Munneer, ed., Elsevier, 2004.

(10) Schmid B. and Wehrli C., *Appl. Opt.* **34**, 4500-4512, 1995.

(11) Holben B.N., et al., *Rem. Sens. Env.* **66**, 1-16, 1998.

(12) Smirnov A., et al., *Rem. Sens. Env.* **73**, 337-349, 2000.

(13) O'Neill N.T., et al., *Geophys. Res. Lett.* **27**, 3333-3336, 2000.

(14) Maxwell E.L., *Solar Energy* **62**, 263-279, 1998.

(15) Maxwell E.L. and Myers D.R., *Daily estimates of aerosol optical depth for solar radiation models*, Proc. Solar '92, American Solar Energy Society, 323-327, 1992.

(16) Gueymard C., *Solar Energy* **43**, 253-265, 1989.

(17) Molineaux B., et al., *Appl. Opt.* **37**, 7008-7018, 1998.

(18) Gueymard C.A., *High performance model for clear-sky irradiance and illuminance*, Proc. Solar 2004, American Solar Energy Society, Portland, OR, 2004.

(19) Gueymard C., *Solar Energy* **50**, 385-397 (Erratum: **51**, 525), 1993.

(20) Elterman L., *Appl. Opt.* **9**, 1804-1810, 1970.

(21) Sasano Y., *Appl. Opt.* **35**, 4941-4952, 1996.

(22) Hayasaka T., et al., *Appl. Opt.* **37**, 961-970, 1998.

(23) Nyeki S., et al., *Geophys. Res. Lett.* **27**, 689-692, 2000.

(24) Rössler F., *Arch. Met. Geoph. Biokl.* **B27**, 69-74, 1979.

(25) Ingold T., et al., *J. Geophys. Res.* **106D**, 27537-27554, 2001.

(26) Liu L., et al., *J. Quant. Spectros. Radiat. Transf.* **88**, 97-109, 2004.

(27) Diner D.J., et al., *IEEE Trans. Geosci. Rem. Sens.* **36**, 1072-1087, 1998.

(28) Myers D.R., et al., *Analysis of broadband model performance for an updated National Solar Radiation Database in the United States of America*, Proc. Solar World Congress, International Solar Energy Society, 2005.

(29) Gueymard C., et al., *China's dust affects solar resource in the U.S.: A case study*, Proc. Solar 2000, American Solar Energy Society, 2000.